Supplemental information

An airway organoid-based screen identifies

a role for the HIF1α-glycolysis axis

in SARS-CoV-2 infection

Xiaohua Duan, Xuming Tang, Manoj S. Nair, Tuo Zhang, Yunping Qiu, Wei Zhang, Pengfei Wang, Yaoxing Huang, Jenny Xiang, Hui Wang, Robert E. Schwartz, David D. Ho, Todd Evans, and Shuibing Chen

Figure S1

A

B

MUC5AC DAPI

P63 DAPI

C

CDK1 *TOP2A* *TP63* *KRT17*

D

SFTPD *SFTPC* *NAPSA*
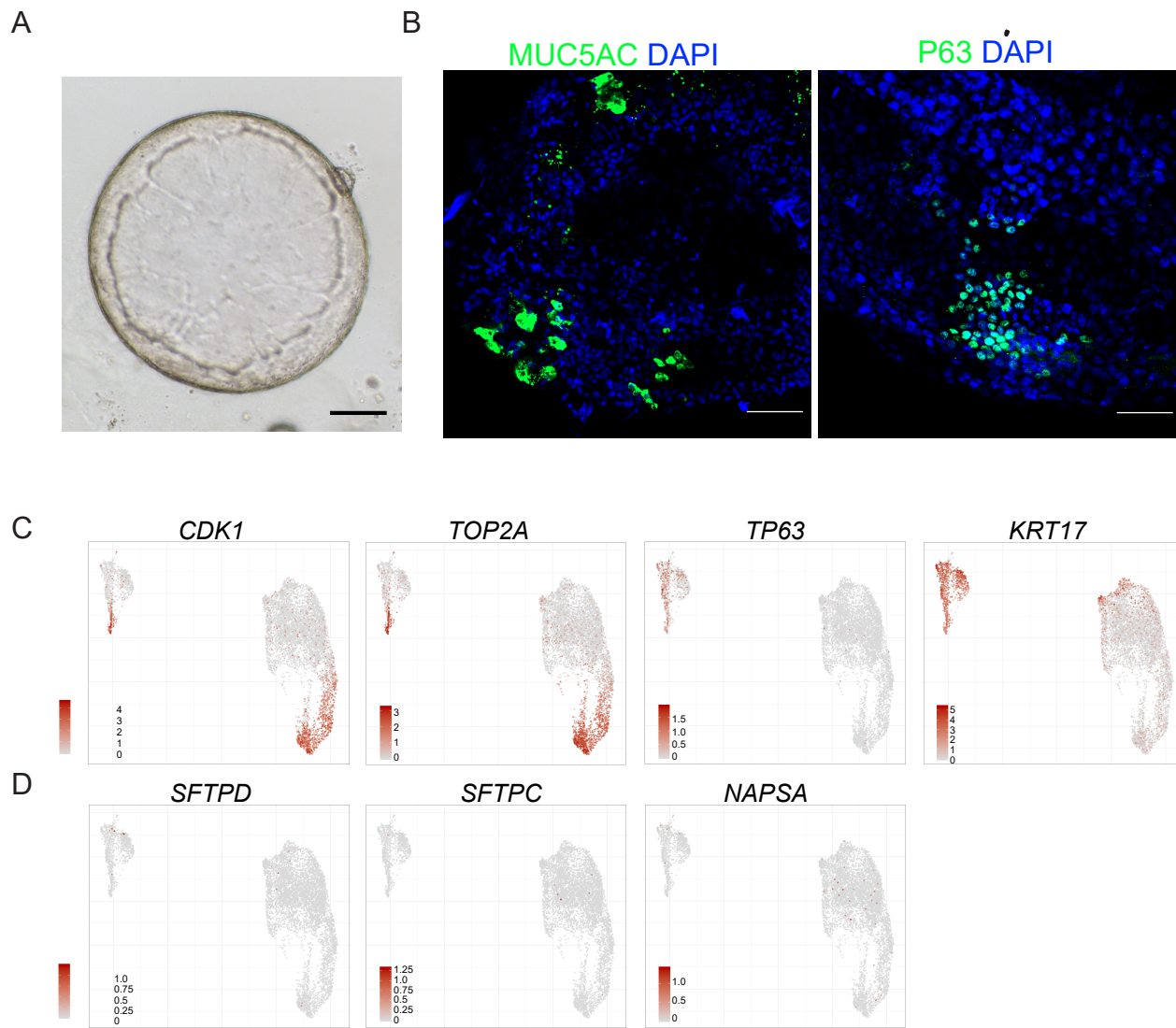
Figure S1. Derivation and Characterization of hPSC-AOs.

(A) Phase contrast image of a representative hPSC-ASs. Scale bar = 400 μm.

(B) Representative confocal images of goblet cell marker MUC5AC and basal cell marker P63 in

hPSC-AOs. DAPI stains nuclei. Scale bar = 100 μm.

(C and **D)** UMAP showing the expression levels of (C) hPSC-AOs cell markers and (D) alveolar

epithelial type 2 cell markers**.** Related to Figure 1.

Figure S2

A
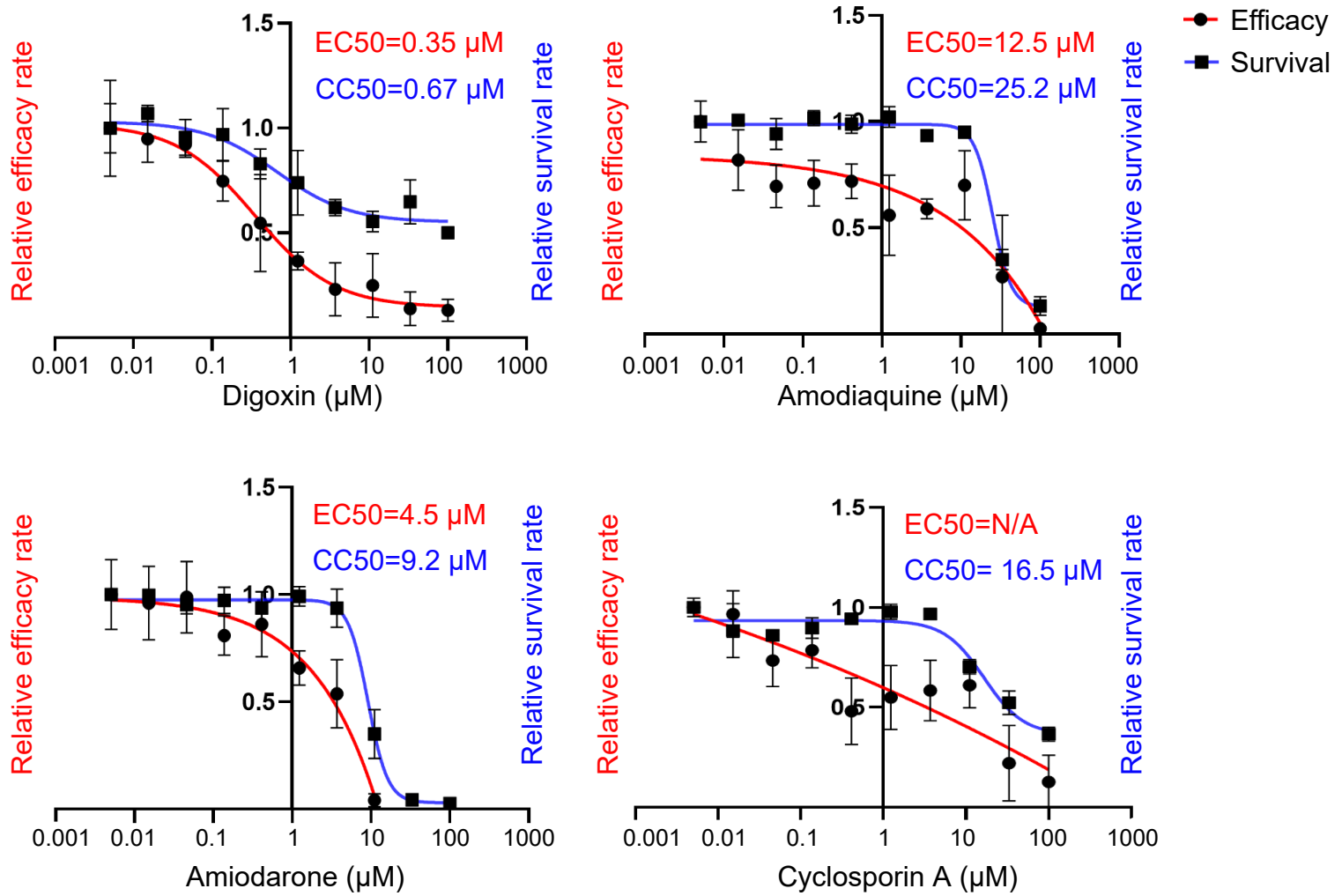
B
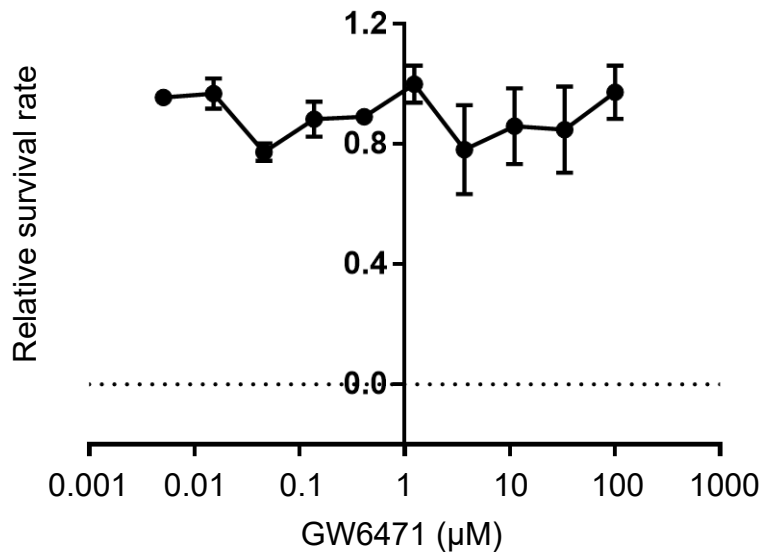
Figure S2. Confirmation of hit compounds from high content screen.

(A) Efficacy and toxicity curves of hit compounds identified from the high content screen.

(B) Cell survival curve of GW6471 on hPSC-AOs.

Data is presented as mean ± SEM. N=3 biological replicates. Related to Figure 3.

Figure S3

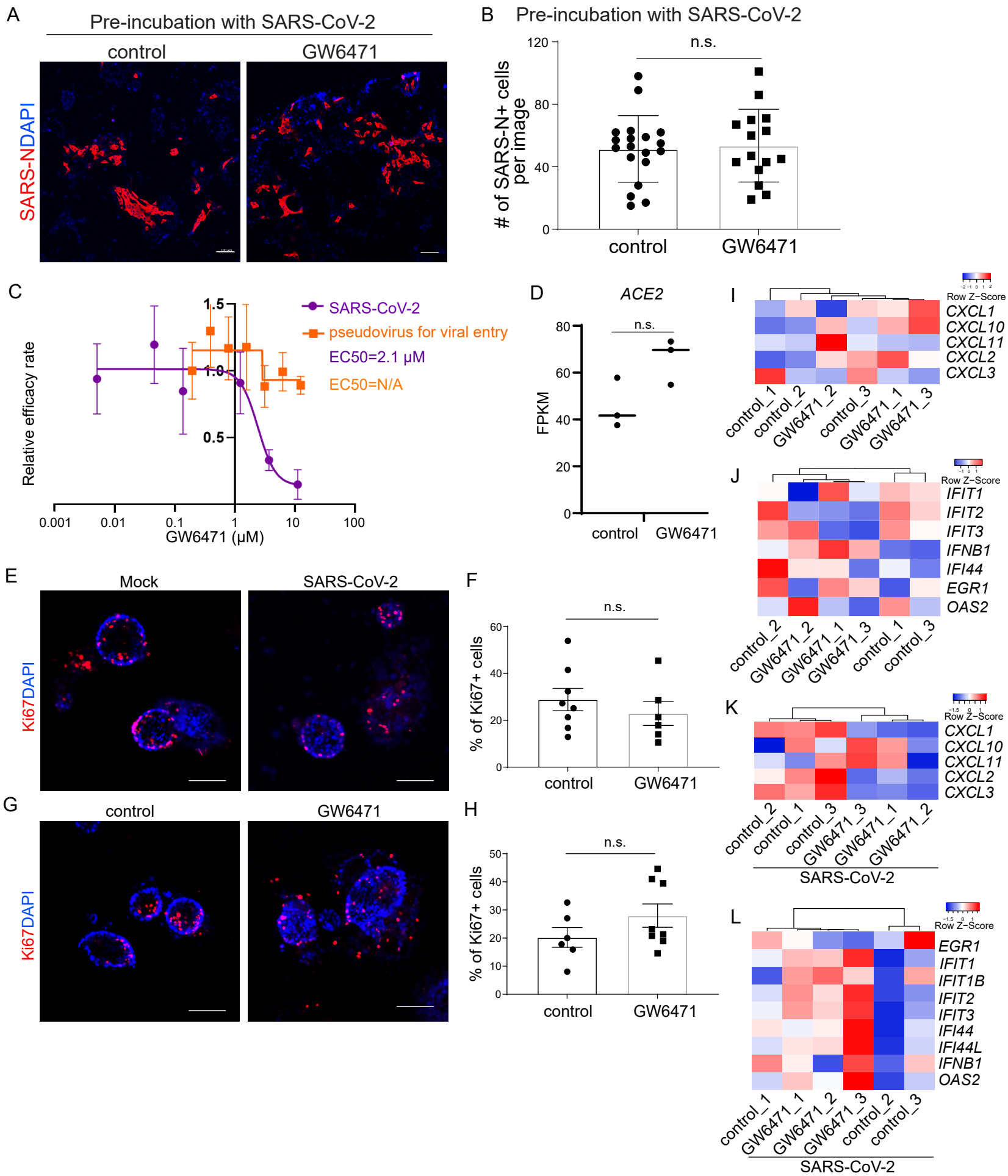**A** Pre-incubation with SARS-CoV-2
control | GW6471
SARS-NDAPI

B Pre-incubation with SARS-CoV-2
n.s.
# of SARS-N+ cells per image
control | GW6471

C
Relative efficacy rate
GW6471 (µM)
- SARS-CoV-2
- pseudovirus for viral entry
EC50=2.1 µM
EC50=N/A

D *ACE2*
n.s.
FPKM
control | GW6471

E Ki67DAPI
Mock | SARS-CoV-2

F n.s.
% of Ki67+ cells
control | GW6471

G Ki67DAPI
control | GW6471

H n.s.
% of Ki67+ cells
control | GW6471

I Row Z-Score
CXCL1, CXCL10, CXCL11, CXCL2, CXCL3
control_1, control_2, GW6471_2, control_3, GW6471_1, GW6471_3

J Row Z-Score
IFIT1, IFIT2, IFIT3, IFNB1, IFI44, EGR1, OAS2
control_2, GW6471_2, GW6471_1, GW6471_3, control_1, control_3

K Row Z-Score
CXCL1, CXCL10, CXCL11, CXCL2, CXCL3
control_2, control_1, control_3, GW6471_3, GW6471_1, GW6471_2
SARS-CoV-2

L Row Z-Score
EGR1, IFIT1, IFIT1B, IFIT2, IFIT3, IFI44, IFI44L, IFNB1, OAS2
control_1, GW6471_1, GW6471_2, GW6471_3, control_2, control_3
SARS-CoV-2

Figure S3. The impact of GW6471 on viral cycle and host AOs.

(**A** and **B**) Representative confocal images (A) and quantification (B) at 48 hpi of SARS-N^{+} cells of hPSC-AOs, infected with SARS-CoV-2 which was pre-incubated with GW6471 or control (MOI=0.2). Scale bar = 100 μm. Data is presented as mean ± SEM. N=3 biological replicates.

(**C**) Efficacy curves of GW6471 on SARS-CoV-2 or pseudovirus. Data is presented as mean ± SD. N=3 biological replicates.

(**D**) FPKM value of ACE2 of control or 10 μM GW6471 treated hPSC-AOs at 48 hpi (MOI=0.2). Data is presented as mean ± SD. N=3 biological replicates.

(**E** and **F**) Representative confocal images (E) and quantification (F) of Ki67^{+} cells of mock or SARS-CoV-2 infected (MOI=0.2) hPSC-AOs. Scale bar = 100 μm. Data is presented as mean ± SEM. N=3 biological replicates.

(**G** and **H**) Representative confocal images (G) and quantification (H) of Ki67^{+} cells of GW6471 or control treated hPSC-AOs (MOI=0.2). Scale bar = 100 μm. Data is presented as mean ± SEM. N=3 biological replicates.
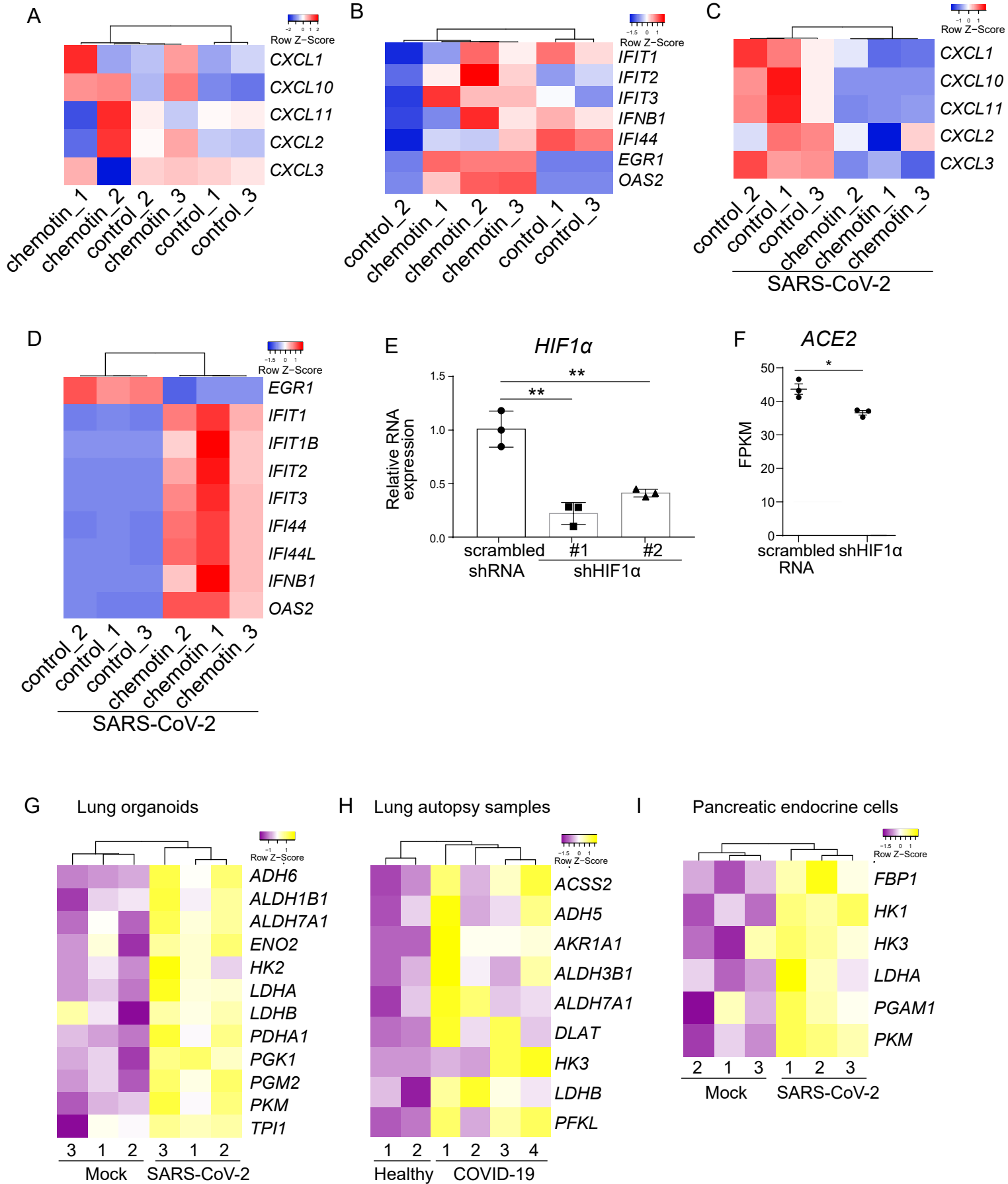
(**I** and **K**) Heatmap of chemokine (I) and interferon (K) expression of GW6471 or control treated hPSC-AOs in the absence of SARS-CoV-2.

(**J** and **L**) Heatmap of chemokine (J) and interferon (L) expression of GW6471 or control treated hPSC-AOs in the presence of SARS-CoV-2 (MOI=0.2).

P values were calculated by unpaired two-tailed Student's t test.

Related to Figure 4.

Figure S4

A

CXCL1
CXCL10
CXCL11
CXCL2
CXCL3

chemotin_1, chemotin_2, control_2, chemotin_3, control_1, control_3

B

IFIT1
IFIT2
IFIT3
IFNB1
IFI44
EGR1
OAS2

control_2, chemotin_1, chemotin_2, chemotin_3, control_1, control_3

C

CXCL1
CXCL10
CXCL11
CXCL2
CXCL3

control_2, control_1, control_3, chemotin_2, chemotin_1, chemotin_3

SARS-CoV-2

D

EGR1
IFIT1
IFIT1B
IFIT2
IFIT3
IFI44
IFI44L
IFNB1
OAS2

control_2, control_1, control_3, chemotin_2, chemotin_1, chemotin_3

SARS-CoV-2

E

HIF1α

Relative RNA expression

scrambled shRNA, #1, #2

shHIF1α

** **

F

ACE2

FPKM

scrambled RNA, shHIF1α

*

G Lung organoids

ADH6
ALDH1B1
ALDH7A1
ENO2
HK2
LDHA
LDHB
PDHA1
PGK1
PGM2
PKM
TPI1

3, 1, 2, 3, 1, 2

Mock, SARS-CoV-2

H Lung autopsy samples

ACSS2
ADH5
AKR1A1
ALDH3B1
ALDH7A1
DLAT
HK3
LDHB
PFKL

1, 2, 1, 2, 3, 4

Healthy, COVID-19

I Pancreatic endocrine cells

FBP1
HK1
HK3
LDHA
PGAM1
PKM

2, 1, 3, 1, 2, 3

Mock, SARS-CoV-2

Figure S4. RNA-seq analysis.

(**A** and **B**) Heatmap of chemokine (A) and interferon (B) expression of chetomin or control treated hPSC-AOs in the absence of SARS-CoV-2.

(**C** and **D**) Heatmap of chemokine (C) and interferon (D) expression of chetomin or control treated hPSC-AOs in the presence of SARS-CoV-2 (MOI=0.2).

(**E**) Relative HIF1α mRNA expression in hPSC-AOs expressing shHIF1α or scrambled shRNA. Data is presented as mean ± SEM. N=3 biological replicates.

(**F**) FPKM value of ACE2 of control or chetomin-treated hPSC-AOs at 48 hpi (MOI=0.2). Data is presented as mean ± SD. N=3 biological replicates.

(**G**)Heatmap of glycolysis pathway associated genes in SARS-CoV-2 infected hPSC-lung organoids (GSE155241).

(**H**) Heatmap of glycolysis pathway associated genes in autopsy samples of COVID-19 patients (GSE155241).

(**I**) Heatmap of glycolysis pathway associated genes in SARS-CoV-2 infected pancreatic endocrine cells (GSE147903).

P values were calculated by unpaired two-tailed Student's t test. Related to Figure 4 and Figure 6.

Table S3. shRNAs for HIF1α knockdown. Related to Figure 4.

Scrambled shRNA	*GCACTACCAGAGCTAACTCAGATAGTACT*
shHIF1α_#1	*AGCTTGCTCATCAGTTGCCACTTCCACAT*
shHIF1α_#2	*TACGTTGTGAGTGGTATTATTCAGCACGA*

Table S5. Antibodies used for immunocytochemistry. Related to STAR*METHODS.

Usage	Antibody	Clone #	Host	Catalog #	Vendor	Dilution
Immunocytochemistry	Human ACE-2 Antibody	Polyclonal	Goat	AF933	R&D Systems	1:200
Immunocytochemistry	CDX2	CDX2-88	Mouse	MU392A-UC	Biogenex	1:500
Immunocytochemistry	Cytokeratin-20	SPM140	Mouse	sc-56522	Santa Cruz	1:100
Immunocytochemistry	FOXJ1	2A5	Mouse	14-9965-82	Thermo Fisher Scientific	1:100
Immunocytochemistry	acetyl-alpha tubulin	6-11B-1	Mouse	MABT868	Sigma-Aldrich	1:3000
Immunocytochemistry	acetyl-alpha tubulin	D20G3	Rabbit	5335	Cell Signaling	1:3000
Immunocytochemistry	MUC5AC	45M1	Mouse	MA5-12178	Thermo Fisher Scientific	1:100
Immunocytochemistry	P63	4A4	Mouse	CM163A	Biocare	1:100
Immunocytochemistry	SARS-CoV/SARS-CoV-2 Nucleocapsid Antibody	R001	Rabbit	40143-R001	Sino Biological	1:200
Immunocytochemistry	Ki67 Antibody	SP6	Rabbit	RM-9106-S1	Thermo Fisher Scientific	1:500
Immunocytochemistry	Donkey anti-Mouse IgG (H+L) Cross-Adsorbed Secondary Antibody, Alexa Fluor 488	Polyclonal	Donkey	#A-21202	Thermo Fisher Scientific	1:500

Immunocytochemistry	Donkey anti-Rabbit IgG (H+L) Secondary Antibody, Alexa Fluor 594	Polyclonal	Donkey	#A-21207	Thermo Fisher Scientific	1:500
Immunocytochemistry	Donkey anti-Goat IgG (H+L) Cross-Adsorbed Secondary Antibody, Alexa Fluor 647	Polyclonal	Donkey	#A-21447	Thermo Fisher Scientific	1:500
Immunocytochemistry	Donkey anti-Goat IgG Secondary Antibody, Alexa Fluor 594	Polyclonal	Donkey	A32816	Thermo Fisher	1:500
Immunocytochemistry	Donkey anti-Rabbit IgG Secondary Antibody, Alexa Fluor 647	Polyclonal	Donkey	A32795	Thermo Fisher	1:500

Table S6. Primers used for qRT-PCR. Related to STAR*METHODS.

Primer name	Sequence
ACTB-Forward	*CGTCACCAACTGGGACGACA*
ACTB-Reverse	*CTTCTCGCGGTTGGCCTTGG*
SARS-CoV-2-TRS-L	*CTCTTGTAGATCTGTTCTCTAAACGAAC*
SARS-CoV-2-TRS-N	*GGTCCACCAAACGTAATGCG*
HIF1α-Forward	*TATGAGCCAGAAGAACTTTTAGGC*
HIF1α-Reverse	*CACCTCTTTTGGCAAGCATCCTG*